Genetic Analysis of MRL-*lpr* Mice: Relationship of the *Fas* Apoptosis Gene to Disease Manifestations and Renal Disease-modifying Loci

By Mark L. Watson,*‡ Jaya K. Rao,* Gary S. Gilkeson,*§ Philip Ruiz,‖ Eva M. Eicher,¶ David S. Pisetsky,*‡§ Akio Matsuzawa,** Julie M. Rochelle,*‡ and Michael F. Seldin*‡

*From the *Autoimmune Genetics Center, Division of Rheumatology, Department of Medicine, and the ‡Department of Microbiology and Immunology, Duke University Medical Center, Durham, North Carolina 27710; the §Medical Service, Durham Veterans Administration Hospital, Durham, North Carolina 27705; the ‖Department of Pathology, University of Miami, Miami, Florida 33101; ¶The Jackson Laboratory, Bar Harbor, Maine 04609; and the **Laboratory Animal Research Center, and the Institute of Medical Sciences, University of Tokyo, Tokyo 108, Japan*

Summary

In MRL mice, the mostly recessive *lpr* mutation results in both the accumulation of $CD4^-$, $CD8^-$,$CD3^+$ T cells in lymphoid tissue and many features of generalized autoimmune disease, including immune complex glomerulonephritis. To positionally clone the *lpr* mutation and analyze the effects of background genes, backcross offspring were examined from the cross: (MRL/MpJ-*lpr* × CAST/Ei)F_1 × MRL/MpJ-*lpr*. The *lpr* gene was found to be closely linked to a mouse chromosome 19 marker defined by a variation of a *Fas* gene restriction fragment. Our results identified differences in RNA expression and differences in the genomic organization of the *Fas* gene between normal and *lpr* mice, and confirm the recent report that a mutation in the *Fas* apoptosis gene is the *lpr* mutation. However, our results also indicate that the *Fas* gene is expressed in spleen cells from normal mice, and spleen and lymph node cells from mice with a second mutation at the *lpr* locus (lpr^{cg}). Together these results suggest that altered *Fas* transcription results in the failure of lymphocytes to undergo programmed cell death and may lead to an altered immune cell repertoire. This mechanism may explain certain central and peripheral defects in tolerance that are present in autoimmune disease. The current study also demonstrates the profound effect of background genes on the degree of nephritis, lymphadenopathy, and anti-DNA antibody production. Of major note, our studies suggest the identification of chromosomal positions for genes that modify nephritis. Analysis of the backcross mice for markers covering most of the mouse genome suggests that over 50% of the variance in renal disease is attributable to quantitative trait loci on mouse chromosomes 7 and 12. Moreover, this study provides a model for dissecting the complex genetic interactions that result in manifestations of autoimmune disease.

The pathogenesis of generalized autoimmune disease is determined in large part by genetic predisposition. Studies of families with either SLE or Sjogren's disease have demonstrated the importance of heredity and suggest that multiple genetic factors result in a variety of clinical features (1). Although animal models with single gene defects would provide the simplest models to study the role of non-MHC genes in the development and/or potentiation of autoimmunity, a more in-depth analysis indicates that the manifestation of disease results from a complex interaction of genes (reviewed in reference 2). This study provides insight into a single gene defect (*lpr*) and develops an approach to dissect the genetic basis of non-MHC-mediated immunopathogenesis of autoimmune disease.

Single gene defects that lead to or accelerate autoimmune disease include the mouse autosomal recessive mutation *lpr* (lymphoproliferation) (3, 4) that was recently mapped to mouse chromosome (Chr)[1]19 (5). MRL/MpJ mice homozygous for the *lpr* mutation produce large amounts of anti-DNA antibodies, and develop massive lymphadenopathy, se-

[1] *Abbreviations used in this paper:* Chr, chromosome; ds, double stranded; RFLP, restriction fragment length polymorphism; ss, single stranded; QTL, quantitative trait locus.

vere immune complex nephritis, and synovitis (reviewed in references 2 and 6). MRL mice without the *lpr* mutation develop a late onset autoimmune syndrome suggesting that *lpr* accelerates rather than causes disease (2). This suggestion is further supported by the finding that laboratory strain mice that carry the *lpr* mutation develop much less profound manifestations of autoimmune disease than MRL-*lpr* mice (7). Homozygous *lpr* mice are phenotypically similar to mice homozygous for the non-allelic *gld* (generalized lymphproliferative disease) mutation (8), and the compound *lpr*/+,*gld*/+ heterozygote is phenotypically normal (2). However, a new mutation at the *lpr* locus, lpr^{cg}, has recently been described that complements *gld* (9). Although mice with the *lpr*, lpr^{cg}, or *gld* mutations may not mimic precisely a specific human autoimmune disease, they nevertheless represent excellent models of SLE with regard to serologic and immunopathologic features of disease (6).

The lymph nodes of most *lpr/lpr* mice are heavily populated with dull Thy-1^+,dull CD5,$CD4^-$,$CD8^-$ cells. These cells have nonclonal rearrangements of TCR genes (8, 10). In addition, the cells have high expression of cell surface antigens CD45(B220), Ly-6, CD44, and PC-1, and absent expression of surface (s)Ig, Th B, and Ia (8). Previous studies also have established that lymph node cells from *lpr/lpr* mice express large amounts of the *myb* proto-oncogene, which is ordinarily only expressed at high levels in the thymus or after mitogenic stimulation of T cells (11). In addition, *lpr/lpr* peripheral T cells display abnormalities in phosphorylation of part of the TCR complex (12). Thus, these cells represent a unique abnormal T cell subset not seen in easily detectable numbers in normal mice. However, these abnormalities may reflect secondary and tertiary events that are part of a cascade resulting from the primary defect. In fact, most studies have failed to show that the expanded double-negative T cell population found in *lpr/lpr* mice has any function (13).

Although the *lpr* mutation derived its name from the hypothesis that it causes lymphoproliferation, subsequent studies have failed to show increased mitotic activity of the abnormal cells in vivo (14). Rather, results have led to the suggestion that the accumulation of the abnormal T cells is derived from a defect in the thymic selection process, because most pre-T cells are destined to die by apoptosis (15). Analysis of mice transgenic for a TCR specific for the H-Y plus self-antigen also has suggested a partial abnormality in negative intrathymic selection (16). Examination of TCR Vβ repertoire in *lpr/lpr* mice similarly has suggested a partial abnormality in positive selection (17, 18).

The current study was initiated in a dual effort to positionally clone the *lpr* mutation and define the effects of background genes in the manifestation of disease. The analyses presented here of linkage relationships, genomic structure, and RNA expression confirm the suggestion of Watanabe-Fukunaga et al. (19) that a mutation in the *Fas* gene is the *lpr* mutation (19). Our results differ from theirs, however, in methodology and in important details concerning *Fas* gene expression. Moreover, our study examines the complex genetics of *lpr*-associated autoimmune disease, and strongly suggests the identification of renal disease modifying loci on Chrs 7 and 12, explaining much of the large variation in renal disease observed in backcross mice homozygous for the MRL/MpJ-*lpr* allele.

Materials and Methods

Mice

MRL/MpJ-*lpr* (MRL-*lpr*), MRL/MpJ-+ (MRL-+), *Mus musculus castaneus* (CAST/Ei), and (MRL-*lpr* × CAST/Ei)F_1 mice were bred at The Jackson Laboratory (Bar Harbor, ME). CBA/KlJms (CBA) and CBA/KlJms-lpr^{cg} (CBA-lpr^{cg}) mice were maintained at the Laboratory Animal Research Center, University of Tokyo. Reciprocal backcross mice produced from mating involving (MRL-*lpr* × CAST/Ei)F_1 and MRL-*lpr* mice were produced at The Jackson Laboratory and maintained along with parental control mice at the Duke University Vivarium barrier facility.

Phenotypic Markers

Three measurements were performed (total lymphoid weight, degree of nephritis, anti-DNA antibody titer) as terminal studies on MRL-*lpr*, (MRL-*lpr* × CAST/Ei)F_1, and the [(MRL-*lpr* × CAST/Ei)F_1 × MRL-*lpr*] interspecific backcross mice at 20 wk of age. To minimize the variance in the genetically identical parental mice, both the lymphoid mass and nephritis index were expressed as log transformations. The terms LPR and non-LPR phenotype are used within the manuscript to refer to mice that have phenotypes characteristic of MRL-*lpr* (*lpr/lpr*) or (MRL-*lpr* × CAST/Ei)F_1 (*lpr/+*) mice, respectively.

Lymphoid Mass Index. This value represents the $\log_{10}$ of the total lymphoid (lymph node plus spleen) weight (in grams) plus a constant of 0.97. The constant was added to minimize the effect of small variation in weight measurements among phenotype-negative animals. The addition of this constant before log transformation yields a minimum value of zero for this index.

Nephritis Index. Kidney sections were stained with hematoxylin and eosin and the histopathology assessed by a single observer. This nephritis index represents the $\log_{10}$ of the additive scores of kidney sections graded on a 0–4 scale for intensity of glomerular cell infiltrate, and for the presence of glomerular cellularity, glomerular crescents, glomerular necrosis, tubular casts, and diffuse interstitial infiltrates (where 0 represents no abnormality, and 1, 2, 3, and 4 represent mild, moderate, moderately severe, and severe abnormalities, respectively). Both the MRL-*lpr* parental mice and interspecific backcross mice varied with respect to these individual disease parameters. However, there was no more variability in the backcross mice that had nephritis index values in the range of the MRL-*lpr* parental mice than in the MRL-*lpr* parental mice themselves (data not shown). Thus, it is likely that separate genetic factors are not responsible for the different measurements used to determine the extent of renal disease.

Anti-DNA Antibodies. IgG antibodies to single-stranded (ss) and double-stranded (ds) DNA were assayed by ELISA using calf thymus DNA (Sigma Chemical Co., St. Louis, MO) coated on 96-well polystyrene microtiter plates (Dynatech, Chantilly, VA) as previously described (20). Briefly, sera were added in serial dilutions in PBS-Triton X-100 (PBS-T) (Sigma Chemical Co.) followed by goat anti-mouse IgG peroxidase (Sigma Chemical Co.) diluted in PBS-T. After incubation, trimethylene-bis (4-formylpyridinium) (TMB) substrate (Sigma Chemical Co.) was added, and the absorbancies at 380 nm were determined on a plate reader. ssDNA used

as antigen was obtained by boiling for 10 min before immediate immersion in ice. dsDNA was obtained by treating the DNA preparation with S_1 nuclease. The dsDNA preparation used showed no reactivity by ELISA using a mouse mAb specific for ssDNA.

Southern Blot Hybridization

DNA from backcross mice was extracted from tissues using standard techniques and digested with restriction endonucleases (Boehringer Mannheim Biochemicals, Indianapolis, IN). 10 μg of each sample was subjected to electrophoresis on 0.9% agarose gels and transferred to Nytran membranes (Schleicher & Schuell, Inc., Keene, NH). Hybridization of probes onto membranes was accomplished at 65°C and washed under stringent conditions (21) for mouse probes (0.2× SSC at 65°C), and reduced stringency (0.5× SSC at 55°C) for human probes.

Hybridization Probes

All probes were labeled by a hexanucleotide technique with α-[^{32}P]dCTP (3,000 Ci/mmol; New England Nuclear, Boston, MA) using an oligolabeling kit and protocol from Pharmacia Fine Chemicals (Piscataway, NJ). 97 clones that define 108 loci were used to establish informative markers on each mouse autosome. The clones used for specifically cited chromosomal markers are listed in Table 1. The unpublished clones included: L15 for *Lyw-57* (lymphocyte antigen workshop-57, kind gift of P. Cohen, University of North Carolina, Chapel Hill, NC); bMT008 for *D12Sel1* (DNA segment, Chr 12, Seldin-1), a clone randomly selected from a mouse thymus cDNA library (Stratagene, La Jolla, CA); and MJ55 for *D19Sel3* (DNA segment, Chr 19, Seldin-3), a genomic clone derived from a flow sorted mouse Chr 19 library (38). In addition, several clones were derived by PCR amplification of *Fas* sequences from a mouse thymus cDNA library (Stratagene). Clones include: FasL1R2, a 3′ PCR-amplified probe that contains bp 646–1,405 of the published cDNA sequence (39); FasL2S2, a 5′ PCR-amplified probe that included bp 32–239; and FasS1S9, a PCR-amplified probe that includes bp 220–665. A γ-actin clone (40) was used as a control for Northern blot analysis.

Genomic and cDNA inserts from each clone were prepared by restriction endonuclease digestion and gel purification, or generated by PCR using oligonucleotide primers derived from plasmid sequences flanking the insert cloning site. Restriction fragment length polymorphisms (RFLPs) were defined that distinguished the two parental strains, MRL-*lpr* and CAST/Ei; those used in segregation analyses are listed for specifically cited clones in Table 1.

Northern Blot Analysis

Total RNA was prepared from mouse tissues and separated on formaldehyde agarose gels according to standard techniques (21). Briefly, 20 μg of total RNA was loaded onto 1% agarose gels and separated at 1 V/cm for 14 h, stained with acridine orange, and transferred to Nytran Plus nylon membranes. Northern blots were hybridized under the same conditions as described in Southern Blot Hybridization, and washed at high stringency.

PCR Assays

The presence of the *Fas* gene transcript was assayed using PCR. First, polyadenylated RNA was reverse transcribed with AMV reverse transcriptase (Boehringer Mannheim Biochemicals) and oligo(dT) primers. First-strand cDNA was quantified and subsequently used as template in a 50-μl PCR reaction containing 1–20 ng of cDNA, 1.0 μM of primers, 200 μM dNTPs, 10 mM Tris-HCl, pH 8.3, 50 mM KCl, and 1.25 U ampliTaq polymerase (Perkin Elmer Cetus, Norwalk, CT). Primers used spanned nucleotides 646–675 (L1), 1385–1405 (R2), 32–52 (L2), 239–220 (S2), 220–239 (S1), and 470–451 (S4) of the published mouse *Fas* sequence (40). The standard PCR cycling profile consisted of 40 cycles of 94°C for 1 min, 55°C for 1 min, and 72°C for 1 min. PCR samples without template or *Taq* polymerase were irradiated for 3 min with short-wave UV light 5 cm from the source before temperature cycling. 10 μl of the completed PCR reaction was subjected to electrophoresis on 1.5% agarose gels for analysis.

Linkage and Quantitative Trait Locus Analysis

Gene linkage and genetic maps were determined applying the MAPMAKER computer package using the Kosambi mapping function (41). The MAPMAKER QTL computer package developed by Lander and Botstein (42) was used to analyze the backcross data for the presence of renal disease modifying loci. This computer package divides each chromosome into intervals between mapped markers and then calculates the maximum likelihood that a quantitative trait locus (QTL) is present within these intervals. This program examines the intervals between mapped loci and calculates the most likely phenotypic effect if a linked QTL is present. A logarithm of odds (LOD) score is calculated that reflects the strength of evidence for the presence of a QTL. The program also computes the proportion of variance that can be explained by the putative QTL. Several considerations are important in determining the appropriate level of significance, including map length and interval size. For the current study, which examined ~1,100 cM at a median interval of ~12 cM, a LOD of >2.5 was determined to correspond to an overall false-positive rate of <5% (see reference 42).

Results

Close Linkage of the Fas Gene and the lpr Mutation. To confirm the chromosomal assignment of the *lpr* gene and further define linkage relationships necessary for positional cloning, (MRL-*lpr* × CAST/Ei)F_1 × MRL-*lpr* backcross mice were analyzed. CAST/Ei, an inbred strain derived from *Mus musculus castaneus* mice, rather than an inbred laboratory strain, was chosen as the second parent to enhance the identification of variant genetic markers. The phenotype of individual mice (LPR vs. non-LPR) was determined at 20 wk of age by measurement of lymph node plus spleen weight (lymphoid mass) and anti-dsDNA autoantibody levels. These segregation analyses indicated that the expression of the *lpr* gene was influenced by background genes. For example, only 48 of 182 backcross mice had lymphoid mass index values within 2 SD of the mean of MRL-*lpr* parental mice (compared with 17 MRL-*lpr* parental mice similarly housed, each of which had values within 2 SD). This number (48) is significantly less than the expected number of backcross mice (91) predicted to be *lpr* homozygotes ($\chi^2 = 40.6$, $p < 0.001$, 1 degree of freedom [d.f.]). Conversely, 137 of 182 backcross mice had at least modest lymphadenopathy (compared with 24 [MRL-*lpr* × CAST/Ei]F_1 mice similarly housed), significantly greater than the expected number of backcross mice (91) predicted to have no lymphadenopathy for a single Mendelian recessive gene ($\chi^2 = 46.5$, $p < 0.001$, 1 d.f.). Nevertheless, 84 of 182 backcross mice could be classified as having the LPR or the non-LPR phenotype (see below).

Table 1. *List of Clones Used for Linkage Analysis*

Genes	Locus	Clone	Reference	Restriction enzyme	MRL-*lpr* bands	CAST/Ei bands
					kb	
β-1 adrenergic receptor	*Adrb-1*	β-1	22	TaqI	2.3	2.1
DNA segment, mouse Chr 12, New York University 3	*D12Nyu3*	M13p20-1	23	EcoRI	6.8	6.0
DNA segment, mouse Chr 12, Seldin 1	*D12Sel1*	bMT008	This report	MspI	4.1	4.6
DNA segment, mouse Chr 19, Seldin 3	*D19Sel3*	MJ55	This report	TaqI	7.2	4.6
Epidermal growth factor binding protein	*Egfbp*	MB2-12A	24	TaqI	9.4, 6.2	9.8, 8.5
Fas antigen	*Fas*	FasL1R2	This report	TaqI	1.4	2.1
Glucagon	*Gcg*	pshgluI	25	TaqI	1.8	2.5
High mobility group protein 14–related sequence 7	*Hmg14-rs7*	pM14c	26	TaqI	–*	1.9*
Insulin degrading enzyme	*Ide*	Ide-pSRalph a	27	TaqI	6.6	5.4
Ig heavy chain	*Igh*	pCμ	28	TaqI	11.0, 5.0	6.6, 4.0
Insulin 2	*Ins-2*	pB12MI	29	MspI	2.2	1.9
Insulin 2–related sequence 1	*Ins-2rs1*	pB12MI	29	BamHI	6.0	2.2
Integration site 2	*Int-2*	BK4	30	BamHI	3.0	2.4
Laminin b 1	*Lamb-1*	PpE386	31	MspI	5.0	2.6
Lymphocyte antigen, workshop-57	*Lyw-57*	L15	Unpublished clone (kind gift of P. Cohen)	BamHI	6.8	5.0
Membrane metallo-endopeptidase	*Mme*	CD10cDNA	32	MspI	12.0	4.3
Oxysterol binding protein	*Osbp*	pB+2.5	33	TaqI	8.0	2.4
Octamer-specific DNA binding protein 2	*Otf-2*	Pac-3-1	34	TaqI	3.8	2.3
Protein kinase C, γ	*Pkcg*	phPKC-γ	35	TaqI	4.4, 2.8	2.6, 4.2
Pro-opiomelanocortin gene 2	*Pomc-2*	Pomc cDNA	36	MspI	1.8	2.2
Ribosomal protein L18-related sequence 9	*Rpl18-rs9*	pL18	37	TaqI	–*	2.8*

* These clones detect multiple pseudogenes that segregate to positions on several chromosomes. The informative CAST/Ei restriction fragment is indicated.

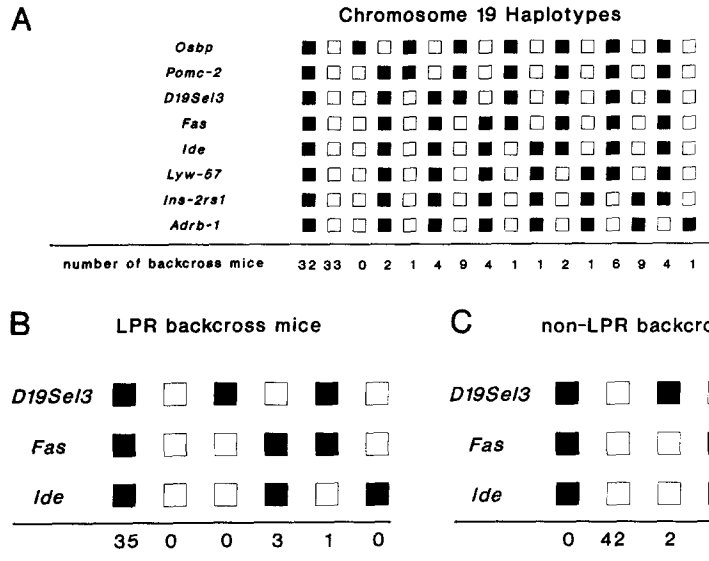

Figure 1. Segregation of the *lpr* mutation with the *Fas* apoptosis gene in (MRL-*lpr* × CAST/Ei)F_1 × MRL-*lpr* backcross mice. For each locus (indicated on the left hand side of each row) the filled boxes represent those mice typed as MRL-*lpr* homozygotes, and the open boxes represent those that typed as the heterozygote F_1 pattern. The number of mice with a given haplotype pattern is shown at the bottom of each column. (*A*) Complete haplotype data for 110 interspecific backcross mice fully typed for mouse Chr 19 markers. (*B* and *C*) Segregation of those mice characterized as LPR and non-LPR phenotype using stringent criteria established by the analysis of backcross mice with nonrecombinant chromosomes. A total of 182 mice were examined, 84 of which fulfilled these criteria.

Since previous studies had localized the *lpr* mutation to mouse Chr 19 (5), we analyzed the segregation of *lpr* using markers that map to this chromosome (*Osbp, Pomc-2, D19Sel3, Fas, Ide, Lyw-57, Ins-2rs1*, and *Adrb-1* [39, 43; and J. M. Rochelle and M. F. Seldin, unpublished data]). Informative RFLPs were determined by analysis of the parental mice (Table 1). Haplotype analysis was then performed for each of the 182 backcross mice, resulting in the genetic map shown in Fig. 1 *A*.

Since the manifestations of autoimmune disease, including lymphadenopathy and anti-dsDNA antibodies, can be influenced by background genes, criteria for LPR and non-LPR phenotype mice were established by analysis of those backcross mice that inherited a nonrecombinant Chr 19 from the F_1 parent (Fig. 1 *A*, columns *1* and *2*), as follows: 32 mice that were homozygotes for all Chr 19 markers derived from the MRL parental genome defined the upper limit of the non-LPR phenotype (lymphoid mass, 0.1 g; and anti-dsDNA antibodies, 1,200), and 33 mice that were heterozygous for all Chr 19 markers defined the lower limit for the LPR phenotype designation (lymphoid mass, 2.5 g; and anti-dsDNA antibodies, 1,750). None of the 84 backcross mice classified as LPR or non-LPR by these criteria inherited a crossover between *lpr* and the *Fas* genes, as shown by haplotype analysis (Fig. 1, *B* and *C*). In addition, when all backcross mice were examined, the MAPMAKER QTL program indicated maximum LOD scores at the *Fas* locus for the measurement of anti-ssDNA (LOD, 17.8), anti-dsDNA (LOD, 30.5), lymphoid mass (LOD, 36.7), and nephritis (LOD 17.4). We conclude that the *lpr* mutation is closely linked to the *Fas* gene.

Analysis of Fas RNA Expression Shows Abnormal Transcription in MRL-lpr Mice. The above mapping data together with the previously defined functional data suggested that an alteration in the *Fas* gene accounts for the phenotypic changes observed in *lpr* homozygous mice. Therefore, *Fas* expression was analyzed by Northern blotting of total RNA purified from several different tissues obtained from MRL-+, MRL-*lpr*, CBA, CBA-*lpr*^{cg}, C3H-+, and C3H-*gld* mice. Using a 3′ Fas cDNA probe (FasL1R2), high-level *Fas* expression was demonstrated in liver from MRL-+ mice, CBA-+, and CBA-*lpr*^{cg} mice (Fig. 2). Moderate expression of the 2.1-kb *Fas* transcript was evident in lymphoid tissue from MRL-+, CBA-+, and CBA-*lpr*^{cg} and C3H-*gld* mice. In contrast, compared with MRL-+ mice, the expression of *Fas* was markedly lower in liver, spleen, and lymph node tissues from *lpr* homozygous mice (Fig. 2). Finally, longer exposures of Northern membranes suggested that a low level of *Fas* gene expression occurred in tissues from *lpr* homozygous mice.

To further analyze the expression of *Fas* in normal and *lpr/lpr* mice, PCR assays were performed from cDNA obtained by reverse transcription of the RNA samples. The PCR amplification of several segments of the *Fas* gene using stringent annealing conditions demonstrated that *Fas* was transcribed in *lpr/lpr* spleen and lymph node cells (Fig. 3). Additionally, quantitative PCR experiments using titrated amounts of cDNA template and a smaller number of PCR cycles suggest that similar amounts of the *Fas* transcript are made in normal and *lpr/lpr* lymphoid tissue (not shown). However, in addition to amplifying fragments of the predicted size, aberrantly sized PCR fragments were obtained with some of the primer pairs (e.g., Fig. 3 *B*). Notably, the PCR primer pairs used to amplify nucleotides 220–470 (S1-S4, 250 bp) and 220–665 (S1-S9, 445 bp) of the published *Fas* cDNA sequence produced additional PCR fragments of 450 bp (Fig. 3 *B*) and 650 bp (not shown), respectively, suggesting that the *Fas* tran-

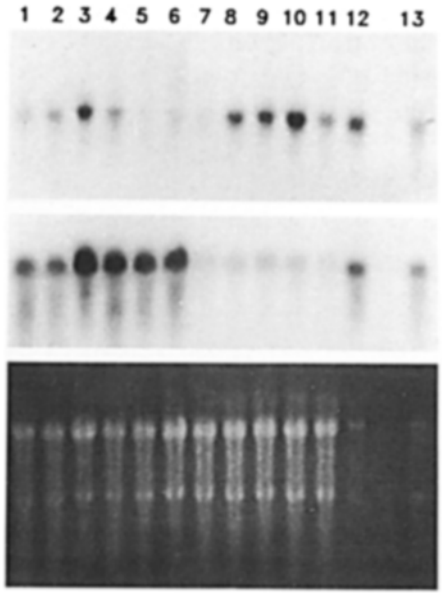

Figure 2. Northern blot hybridization of RNA from MRL-*lpr*, CBA-*lpr*^{cg}, C3H-*gld*, and congenic controls with a 3′ *Fas* apoptosis gene probe (FasL1R2). *Fas* gene expression (*top*) is compared with γ-actin (*Actg*), (*middle*) and acridine orange staining of total RNA (*bottom*) for the following samples: (*1*) CBA-+ spleen, (*2*) CBA-*lpr*^{cg} spleen, (*3*) CBA-*lpr*^{cg} lymph node, (*4*) MRL-+ spleen, (*5*) MRL-*lpr* spleen, (*6*) MRL-*lpr* lymph node, (*7*) MRL-*lpr* liver, (*8*) CBA-+ liver, (*9*) CBA-*lpr*^{cg} liver, (*10*) MRL-+ liver, (*11*) C3H-+ liver, (*12*) C3H-+ thymus, (*13*) C3H-*gld* lymph node. Sizes of the transcripts were 2.1 kb (*Fas*) and 0.7 kb (*Actg*).

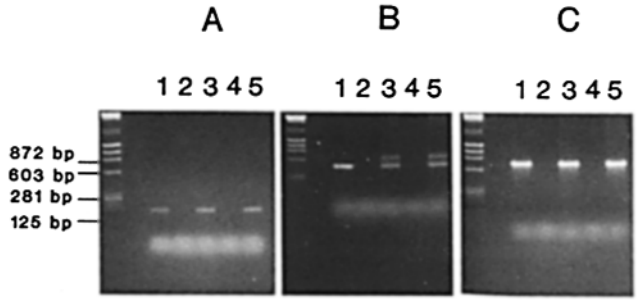

Figure 3. PCR amplification of the *Fas* cDNA segments. The templates were reverse transcribed RNA (20 ng of oligo(dT)-primed cDNA) from MRL-+ spleen (lane *1*), MRL-*lpr* spleen (lane *3*), and MRL-*lpr* lymph node tissue (lane *5*). Three partially overlapping segments of the *Fas* gene were amplified using the following primers: (*A*) L2 and S2 (bp 32–239 of the published sequence; reference 19); (*B*) S1 and S4 (bp 220–470); and (*C*) L1 and R2 (bp 646–1405). Alternate lanes (*2* and *4*) contained PCR control reactions in which no template was added. Results were verified by examination of RNA samples derived from multiple individual mice.

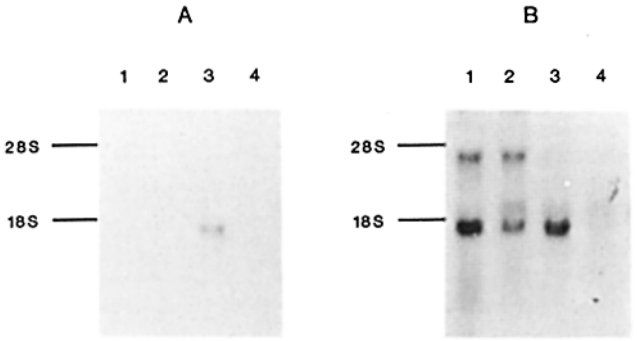

Figure 4. Comparison of *Fas* expression in MRL+ and MRL-*lpr* mice. Probes used for Northern hybridizations were derived using either MRL+ (*A*) or MRL-*lpr* (*B*) cDNA as template for PCR amplification. The region amplified represented a 3′ segment (FasL1R2, bp 646–1405) of the *Fas* gene. In *A*, the wild-type probe detects bands in MRL+ liver (lane *3*), but not MRL-*lpr* spleen, lymph node, or liver (lanes *1*, *2*, and *4*). In *B*, the *lpr* probe detects bands in MRL+ liver (lane *3*), and also hybridizes to transcripts in MRL-*lpr* spleen (lane *1*) and *lpr* lymph node (lane *2*), but does not detect bands in *lpr* liver (lane *4*). Additional higher molecular weight bands are detected by the *lpr*-derived probe in *lpr* spleen and lymph node (lanes *1* and *2*).

scripts in *lpr/lpr* mice contained additional and disparate sequences from the functional *Fas* transcript.

The MRL-*lpr* and MRL+-derived amplified products were gel purified and used as probes for both genomic and Northern blot hybridization. The amplified fragments from both MRL-*lpr* and MRL+ detected the same *Fas* genomic restriction bands that were previously observed using amplified products from a wild-type thymus cDNA library, indicating that the fragments amplified from transcribed sequences were derived from the same region of the genome in both strains (MRL+ and MRL-*lpr*) (data not shown). In contrast, Northern blot analysis showed different expression patterns when *lpr*-derived probes, as compared with wild-type thymus cDNA probes and MRL+-derived probes, were used. For example, when the *lpr*-derived fragment (FasL1R2) was used as a probe prominent transcripts of 2.3 and 4.5 kb were observed in MRL-*lpr* spleen and lymph node tissue (Fig. 4). These differences in hybridization patterns indicate that the fragments amplified from mRNA in *lpr* mice contain sequences not present in transcripts from wild-type mice. These results combined with the PCR results and genomic blot analysis strongly suggest that mRNA processing of the *Fas* gene is different in MRL-*lpr* mice.

Genomic Restriction Analyses Identify a Deletion within the Fas Gene of lpr/lpr mice. Genomic DNA digests were performed to examine whether a structural mutation was present in the *Fas* gene of *lpr/lpr* mice that might explain the differences noted in *Fas* RNA transcripts in cells from *lpr/lpr* mice. DNAs were digested with multiple restriction endonucleases and examined by Southern blot analysis using several *Fas* probes (FasL1R2, FasL2S2, and FasS1S9). The FasS1S9 probe detected multiple differences between MRL-*lpr* and MRL+ DNA samples (e.g., see Fig. 5). Double digests defined a genomic restriction map in MRL+ and MRL-*lpr* DNA (Fig. 5). These analyses indicate that a 1.4-kb fragment of the *Fas* gene is deleted in the *lpr/lpr* mouse and, together with the PCR analyses (see above), suggest that the deletion is probably within a *Fas* intron.

Complex Genetic Interactions Underlie the Manifestations of Autoimmune Disease. The identification of the *Fas* gene as the site of the *lpr* mutation also allows the separation of backcross mice into homozygotes and heterozygotes for *lpr*. The phenotypic characteristics of *lpr/lpr* and *lpr/+* (MRL-*lpr* × CAST/Ei)F_1 × MRL-*lpr* backcross mice were compared with those of the MRL-*lpr* parental and the (MRL-*lpr* × CAST/Ei)F_1 mice (Table 2). The standard deviation for lymphoid mass and renal disease of *lpr* homozygous backcross

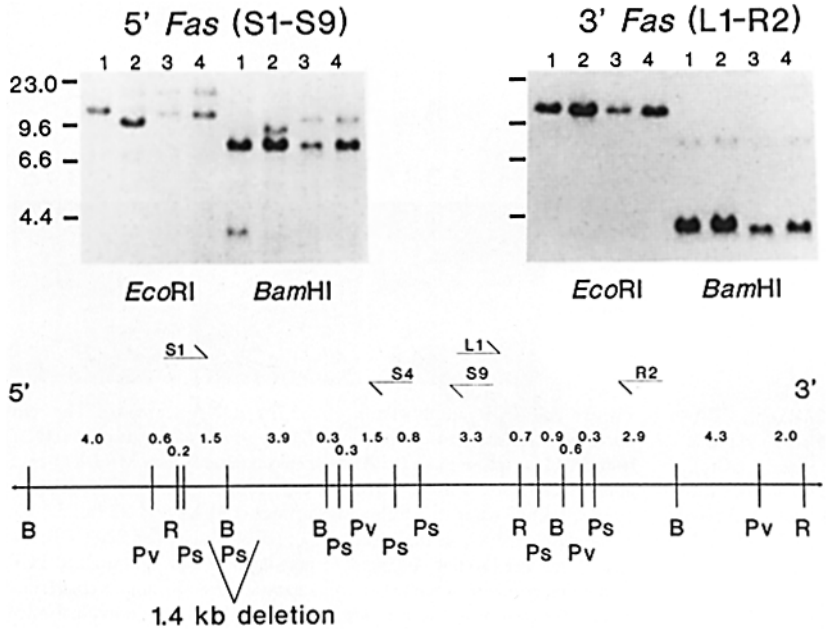

Figure 5. Genomic organization of the *Fas* gene. (*Top*) Representative genomic blot hybridized sequentially to probes derived from the 5′ (FasS1S9, *A*) and the 3′ (FasL1R2, *B*) regions of the *Fas* gene. DNA samples derived from MRL+ (lane *1*), MRL-*lpr* (lane *2*), CBA-+ (lane *3*), and CBA-*lpr*^{cg} (lane *4*) were digested with EcoRI and BamHI. Molecular weight size standards (in kb) are shown to the far left (*top*). (*Bottom*) Restriction map of the genomic region detected by multiple *Fas* probes. Cleavage sites are shown for the restriction enzymes EcoRI (R), BamHI (B), PvuII (Pv), and PstI (Ps). The position of a 1.4-kb deletion associated with the *lpr* mutation is indicated.

Table 2. *Phenotypic Characteristics of MRL-lpr Crosses*

Mice*	Nephritis index‡	Lymphoid mass index	Anti-dsDNA	Anti-ssDNA
MRL-*lpr*	0.97 ± 0.16§ (17)‖	0.72 ± 0.14 (17)	1.047 ± 0.4733 (17)	1.844 ± 0.2306 (17)
F_1	0.10 ± 0.14 (18)	0.02 ± 0.04 (28)	0.060 ± 0.050 (27)	0.3489 ± 0.1638 (27)
BC	0.39 ± 0.35 (183)	0.26 ± 0.30 (182)	0.6567 ± 0.5998 (178)	0.9291 ± 0.4924 (178)
BC-*lpr/lpr*	0.60 ± 0.35 (86)	0.49 ± 0.29 (86)	0.7360 ± 0.5762 (84)	1.254 ± 0.3948 (84)
BC-*lpr/+*	0.19 ± 0.20 (96)	0.06 ± 0.08 (96)	0.2486 ± 0.3600 (93)	0.6459 ± 0.3955 (93)

* The mice examined were the MRL-*lpr*, (MRL-*lpr* × CAST/Ei)F_1 (F_1), and the backcross (MRL-*lpr* × CAST/Ei) × MRL-*lpr* (BC). The interspecific backcross mice were also examined in subsets defined as *lpr/+* and *lpr/lpr* according to their *Fas* locus genotype.
‡ Phenotypic indices are defined in Materials and Methods.
§ SD.
‖ Number of animals examined.

mice was larger than for MRL-*lpr* mice (Table 2). There was also a larger range of values and overlap between *lpr* homozygous and *lpr/+* heterozygous backcross mice for each parameter measured (Fig. 6). Although the distribution of values does not indicate a simple one- or two-gene model, the large variance within *lpr* homozygous backcross mice nevertheless suggests that relatively few genes are responsible for the difference between these mice and parental MRL-*lpr* mice (see references 42 and 44 for relevant discussion).

QTL Suggest Chromosomal Locations of lpr Renal Disease Modifiers. To determine if other loci, in addition to *Fas*, were associated with the inheritance of renal disease, we analyzed

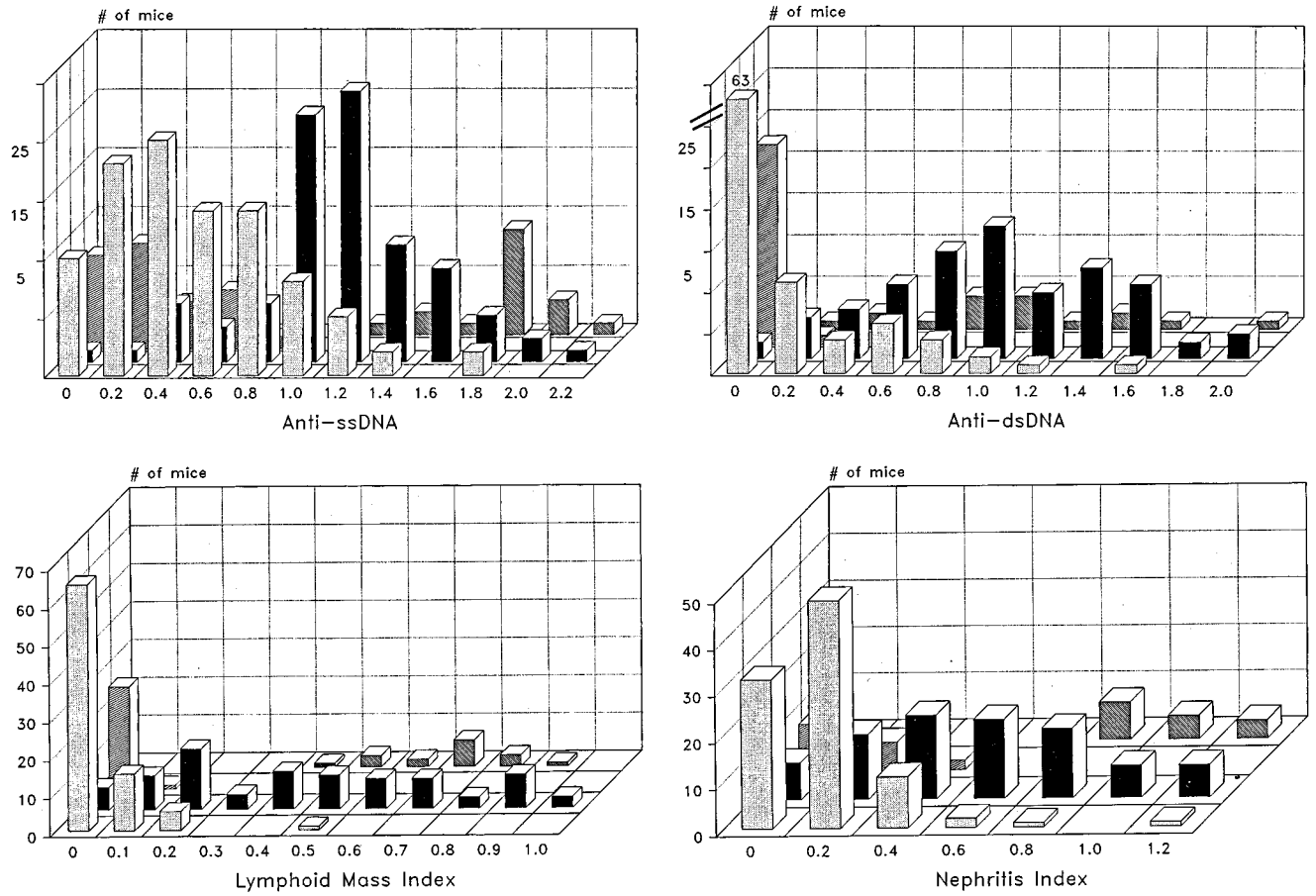

Figure 6. Histogram of the distribution of parental and backcross mice for phenotypic indexes of anti-ssDNA, anti-dsDNA, lymphoid mass, and nephritis. The backcross mice (BC) were divided into *lpr/+* and *lpr/lpr* genotypes as determined by a *Fas* RFLP. The height of each column represents the number of mice with the indicated value. (▨) BC *lpr/+*; (■) BC *lpr/lpr*; (▨) F_1; (▩) MRL-*lpr*.

Table 3. *QTL Analysis of Renal Disease*

Chr	Maximum interval*	LOD‡ score	Markers§	Percent variance‖
	cM			
1	74.3	1.0		3
2	72.4	1.7	*Gcg* (*M. castaneus*)¶	5
3	55.9	1.4	*Mme* (*M. castaneus*)	4
4	70.6	1.3	*Rpl18rs9* (MRL)	4
5	77.7	0.6		
6	70.7	0.6		
7	79.2	3.0 (3.0)**	*Pkcg-Otf-2* (MRL)	8 (24)‡‡
8	39.0	0.0		
9	72.7	0.2		
10	53.5	0.9		
11	62.3	0.1		
12	61.8	2.9 (3.9)**	*D12Nyu3-D12Sel1* (MRL)	10 (38)‡‡
13	61.1	0.0		
14	23.4	0.6		
15	62.0	0.1		
16	31.0	0.1		
17	26.8	0.1		
18	31.4	0.1		
19	43.9	17.4	*Fas* (MRL)	37

* Interval from most proximal to most distal marker that was examined for each chromosome.
‡ Maximum LOD score on each chromosome when the interspecific backcross mice were examined for variance of the renal index.
§ Markers closest to the maximum LOD score are shown for those chromosomes in which a LOD score of at least 1.0 was reached.
‖ The percent variance explained by the putative QTL.
¶ The parental strain associated with disease.
** LOD score for analysis of only backcross mice homozygous for the MRL-*lpr Fas* RFLP.
‡‡ The percent variance explained by the putative QTL when only those backcross mice homozygous for the MRL-*lpr Fas* RFLP were examined.

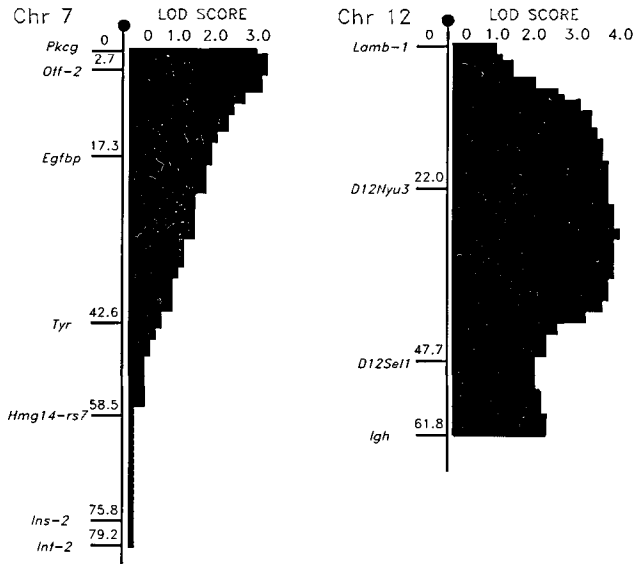

Figure 7. Histogram of LOD score values for renal disease QTL analysis on mouse Chrs 7 and 12.

cosegregation with polymorphic markers on each mouse autosome. X chromosomal loci were not examined since there was no difference in the incidence of renal disease in male and female progeny (data not shown). A total of 108 loci were analyzed that covered between 23 and 79 cM on each autosome (Table 3) and spanned a total of 1,070 cM with only six intervals >25 cM. Comparison with previous genetic maps suggests that these markers cover ~75% of the genome at a resolution of <20 cM (M. F. Seldin, unpublished data). A minimum of 110 backcross mice were typed for all 108 loci, and 182 backcross mice were typed for 60 loci. The MAPMAKER QTL program was utilized to analyze these data for the identification of disease modifying loci (41; see Materials and Methods).

In addition to the region of mouse Chr 19 containing the *Fas* locus, two chromosomal regions, the proximal segment of mouse Chr 7 (*Otf-2, Pkcg*) and the middle segment of mouse Chr 12 (*D12Nyu3, D12Sel1*), were associated with renal disease showing LOD scores of 3.0 and 2.9, respectively (Table 3). The MRL-*lpr* haplotype was overrepresented in those mice with high nephritis indices and under represented in those mice with low nephritis indices. When only those backcross

mice that were *lpr* homozygotes (as determined by *Fas* locus typing) were examined, the LOD score for the Chr 7 loci remained at 3.0 and that for the Chr 12 loci increased to 3.9 (even though the number of mice was reduced from 182 to 86; Table 2 and Fig. 7). Together, this analysis suggests that these two chromosomal regions account for >50% of the variance observed in the *lpr* homozygous backcross mice (Table 3).

Discussion

The current study confirms the conclusion of Watanabe-Fukunaga et al. (19) that the *Fas* gene contains the *lpr* mutation. The *Fas* gene is closely linked to the *lpr* mutation and RNA expression was dramatically altered in tissues from *lpr/lpr* mice. However, in contrast to previous studies (19), the current results indicate that *Fas* mRNA is produced in tissue from MRL-*lpr* mice, albeit of different size transcripts. The PCR results using primers that amplify sequences detecting a *Fas* deletion in genomic DNA from *lpr/lpr* mice also amplify additional DNA fragments from cDNA derived from *lpr/lpr* mice, indicating that the aberrant cDNA contains an additional sequence that is probably intronic. In addition, our genomic restriction site analyses demonstrate that *lpr/lpr* mice have a 1.4-kb deletion within the *Fas* gene. Together, these data suggest that the *Fas* deletion results in the production of nonfunctional mRNA transcripts, possibly due to splicing errors.

The present studies also provide insight into the etiopathogenesis of generalized autoimmunity as well as critical events in T cell differentiation. The *Fas* gene is a type 1 membrane protein with sequence similarity to other members of a putative family of cell surface membrane receptors, including nerve growth factor receptor, CD40, and TNF receptor 1 (TNFR1) (39, 45). The cytoplasmic domain of *Fas*, presumably essential for signal transduction, is most similar to CD40 and TNFR1. Because antibodies directed to *Fas* cell surface antigen induce apoptosis (45), these studies suggest that the profound accumulation of $CD4^-$,$CD8^-$,$CD3^+$ T cells from *lpr/lpr* mice results from escape of these cells from a normal apoptotic process.

A large variety of data suggest that during normal T cell development, both positive and negative selection takes place to eliminate potentially autoreactive cells (15). Although the double-negative cells in MRL-*lpr* mice do not appear to have a functional role (8), the accumulation of these cells suggests that other T cells escape the normal positive and/or negative selection process. Presumed defects in both positive and negative selection have been observed in analysis of *lpr/lpr* mice (16–18). The results of the current study suggest that the expression of the *Fas* gene within the thymus may allow elimination of potentially autoreactive T cells. Perhaps transcriptional control of the *Fas* gene is the first step downstream from the positive and/or negative selection signals.

Although T cell abnormalities have been the major focus of research on the *lpr* mutation, recent adoptive transfer studies indicate that *lpr/lpr* mice have primary defects in both B and T cells (46, 47). Thus, negative and/or positive selection at both the T and B cell levels is probably required to prevent the occurrence of self-reactive cells and autoreactive antibodies. Analysis of *Fas* gene expression during B cell ontogeny potentially can allow delineation of the role of Fas-mediated apoptosis in the determination of peripheral T and/or B cell tolerance.

The phenotypic analysis of interspecific backcross mice segregating for the *lpr* mutation indicates that the manifestations of generalized autoimmune disease in this model result from complex genetic interactions. This result is consistent with previous observations that *lpr* congenic mice (i.e., mice carrying *lpr* mutation on different genetic backgrounds) differ in manifestations of disease (2, 7). In addition, careful serologic analysis has indicated that subtle autoimmune disease can be detected in *lpr*/+ heterozygotes (48). Having identified the likely site of the *lpr* mutation, it was possible to reevaluate the backcross mice that could not be definitively phenotyped as LPR or non-LPR by either anti-DNA antibody levels or degree of lymphadenopathy. These data indicate that several additional genes are necessary for the full manifestation of lymphadenopathy in *lpr* homozygous mice and that *lpr* heterozygotes do have significant disease (up to 2.5 g lymphoid mass) provided certain background genes are present. Similar results were obtained in the analysis of nephritis, anti-ssDNA, and anti-dsDNA antibody levels.

Single gene mutations may have profound effects on the pathophysiology of many different diseases; however, most human and mouse diseases are the result of more complex hereditary factors. The ability to define markers at 10–20-cM intervals throughout the genome has allowed several groups to begin elucidating complex genetic diseases. Initial studies of plant genetic characteristics using these techniques (49, 50) have recently been extended to mammalian systems. Several loci have now been identified as probable disease modifiers in nonobese diabetic mice (51), in salt-sensitive hypertensive rats (52), and in a mouse model for epilepsy (53). The current study adds the MRL-*lpr* autoimmune renal disease to this list. Typing of the (MRL-*lpr* × CAST/Ei)F_1 × MRL-*lpr* backcross mice for markers covering ~75% of the mouse genome indicated an association of renal disease with the MRL parental haplotypes for positions on mouse Chrs 7 and 12. Analysis of only backcross mice that had the *lpr/lpr* genotype (MRL-*lpr* *Fas* homozygotes) showed similar results for a modifying gene being present on Chr 7 and more significant association for another modifying gene being present on Chr 12. At present the position of these QTL on these chromosomes is imprecisely defined. Additional breeding studies in which congenics are established for these regions of the genome will be necessary to further define the location of these *lpr* renal disease modifier loci (*Lrdm-1*, Chr 7; *Lrdm-2*, Chr 12). Although the current data do not exclude the *Igh* locus as a renal disease modifier on mouse Chr 12, the LOD score at this locus was 2.3 compared with the maximum LOD score of 3.9 for a gene located at a more proximal position on Chr 12 (Fig. 7). Potential renal disease modifiers, *Otf-2*, an Ig transcriptional regulator (34), and T cell growth factor B1 (*Tgfb1*), a mediator of inflammation and peripheral tolerance (54, 55), have been mapped close to *Lrdm-1* on mouse Chr 7 (56). In

addition, *Tgfb3* is located in the region of *Lrdm-2* on Chr 12 (57).

None of the other chromosomal markers analyzed had LOD scores >2 (Table 2). Interestingly, one potentially weak renal disease modifier on mouse Chr 3 (LOD, 1.4) is coincident with the location of a very strong NOD modifier (51), raising the possibility that the renal disease observed in *lpr/lpr* mice and diabetes modification in NOD mice may represent a common genetic mechanism. In contrast to the NOD model (51) and previous studies of the NZB model (58, 59), in this study we observed no substantial effect of the MHC or TCR B loci on nephritis.

Finally, this study also may help define the pathogenesis of human generalized autoimmune diseases, such as SLE. Although a profound expansion of double-negative ($CD4^-$, $CD8^-$,$CD3^+$) T cells has not been observed in these patients, the variable expression of the *lpr* homozygous and *lpr* heterozygous genotypes observed in the current study leaves open the possibility that a similar defect in lymphocyte apoptosis may, in part, account for the wide array of autoantibodies that characterize SLE. Furthermore, the localization of disease-modifying genes from mouse studies can be used to predict the chromosomal location of homologous human disease-modifying loci because of conservation of linkage groups between these species (reviewed in reference 60). For autoimmune renal disease, the human chromosomal segments of interest, corresponding to *Lrdm-1* and *Lrdm-2*, are located on the proximal long arm of human Chr 19 and long arm of human Chr 14, respectively. In summary, studying the inheritance of complex diseases in the mouse may help define the complex genetics of human autoimmune disease.

We thank the following individuals for providing clones used in the current study: R. J. Lefkowitz, β-1; P. D'Eustachio, M13p20-1; R. A. Bradshaw, MB2-12A; G. I. Bell, pshglul; M. Bustin, pM14c; R. A. Roth, Ode-pSRalpa; K. B. Marcu, pCμ; B. R. Cullen, pB12MI; C. Dickson, BK4; R. W. Elliott, PpE386; P. Cohen, L15; M. A. Shipp, CD10 cDNA; J. L. Goldstein, pB+2.5; L. M. Staudt, Pac-3-1; A. Ullrich, phPKC-γ; J. Roberts, Pomc cDNA; R. P. Perry, Rpl18. We also thank Dr. K. Johnson and M. Davisson for suggesting the use of Hmg14 and Rpl18 probes to detect multiple loci, T. A. Howard for technical assistance, D. Bennett for secretarial assistance, R. J. Oakey for valuable discussions, E. S. Lander and S. Lincoln for providing the MAPMAKER QTL program, K. Johnson and B. Paigen for critical review of the manuscript, and D. Wolfe and C. W. Stuber for their kind donation of time in assisting in QTL computer analysis.

This work was supported by an Arthritis Foundation Biomedical Research grant (M. L. Watson and M. F. Seldin), National Institutes of Health grants AR-41053 (M. F. Seldin and M. L. Watson), AR-39162 (D. S. Pisetsky), AK-01847 (G. S. Gilkeson), and RR-01183 (E. M. Eicher). D. S. Pisetsky is a member of the Veteran's Administration Medical Research Service. G. S. Gilkeson is a Fellow of the Arthritis Foundation. M. L. Watson is supported by MSTP grant T32 GM-07171. A. Matsuzawa is supported by a Grant-in-Aid for Scientific Research by the Ministry of Education, Science and Culture, Japan (04454185).

Address correspondence to M. F. Seldin, Department of Medicine, Box 3380, Duke University Medical Center, Durham, NC 27710.

Received for publication 10 July 1992.

Note added in proof: Sequencing of *lpr Fas* transcripts confirms that many of these transcripts contain nonexonic sequence. Analysis of additional data indicate an increased LOD score (4.8) for the mouse Chr 12 renal disease QTL.

References

1. Winchester, R.J., and R.G. Lahita. 1987. Genetic susceptibility to systemic lupus erythematosus. *In* Systemic Lupus Erythematosus. R.G. Lahita, editor. John Wiley & Sons, Inc., New York. 81–118.
2. Theofilopoulos, A.N., and F.J. Dixon. 1985. Murine models of systemic lupus erythematosus. *Adv. Immunol.* 37:269.
3. Andrews, B.S., R.A. Eisenberg, A.M. Theofilopoulos, S. Izui, C.B. Wilson, P.J. McConahey, E.D. Murphy, J.B. Roths, and F.J. Dixon. 1978. Spontaneous murine lupus-like syndromes. Clinical and immunopathological manifestations in several strains. *J. Exp. Med.* 148:1198.
4. Murphy, E.D. 1981. Lymphoproliferation (*lpr*) and other single-locus models for murine lupus. *In* Immunologic Defects in Laboratory Animals, Vol. 2. M.E. Gershwin, and B. Berchant, editors. Plenum Publishing Corporation, New York. 143–171.
5. Watanabe, T., Y. Sakai, S. Miyawaki, S. Atsuko, O. Koiwai, and K. Chno. 1991. A molecular genetic linkage map of mouse chromosome 19, including the *lpr*, *Ly-44* and *Tdt* genes. *Biochem. Genet.* 29:325.
6. Cohen, P.L., and R.A. Eisenberg. 1991. *lpr* and *gld*: single gene

models of systemic autoimmunity and lymphoproliferative disease. *Annu. Rev. Immunol.* 9:243.
7. Izui, S., V.E. Kelley, K. Masuda, H. Yoshida, J.B. Roths, and E.D. Murphy. 1984. Induction of various autoantibodies by mutant gene *lpr* in several strains of mice. *J. Immunol.* 133:227.
8. Davidson, W.F., F.J. Dumont, H.G. Bedigian, B.J. Fowlkes, and H.C. Morse III. 1987. Phenotypic, Functional, and Molecular Genetic Comparisons of the Abnormal Lymphoid Cells of C3H-*lpr/lpr* and C3H-*gld/gld* Mice. *J. Immunol.* 136:4075.
9. Matsuzawa, A., T. Moriyama, T. Kaneko, M. Tanaka, M. Kimura, H. Ikeda, and T. Katagiri. 1990. A new allele of the *lpr* locus, lpr^{cg}, that complements the *gld* gene in induction of lymphadenopathy in the mouse. *J. Exp. Med.* 171:519.
10. Mountz, J.D., K.E. Huppi, M.F. Seldin, J.F. Mushinski, and A.D. Steinberg. 1986. T cell receptor expression in autoimmune mice. *J. Immunol.* 137:1029.
11. Mountz, J.D., J.F. Mucinski, D.M. Klinman, H.R. Smith, and A.D. Steinberg. 1984. Autoimmunity and increased c-myb transcription. *Science (Wash. DC).* 226:1087.
12. Samelson, L.E., W.F. Davidson, H.C. Morse III, and R.D, Klausner. 1986. Abnormal tyrosine phosphorylation on T-cell receptor in lymphoproliferative disorders. *Nature (Lond.).* 324:674.
13. Davignon, J.L., R.C. Budd, R. Ceredig, P.F. Piguet, H.R. MacDonald, J.C. Cerottini, P. Vassalli, and S. Izui. 1985. Functional analysis of T cell subsets from mice bearing the *lpr* gene. *J. Immunol.* 135:2423.
14. Raveche, E.S., A.D. Steinberg, A.L. DeFranco, and J.H. Tjio. 1982. Cell cycle analysis of lymphocyte activation in normal and autoimmune strains of mice. *J. Immunol.* 129:1219.
15. Shortman, K., M. Egerton, G.J. Spangrude, and R. Scollay. 1990. The generation and fate of thymocytes. *Immunology.* 2:3.
16. Zhou, T., H. Bluethmann, J. Eldridge, M. Brockhaus, K. Berry, and J.D. Mountz. 1991. Abnormal thymocyte development and production of autoreactive T cells in T cell receptor transgenic autoimmune mice. *J. Immunol.* 147:466.
17. Singer, P.A., R.J. McEvilly, D.J. Noonan, F.J. Dixon, and A.N. Theofilopoulos. 1986. Clonal diversity and T-cell receptor beta-chain variable gene expression in enlarged lymph nodes of MRL-*lpr/lpr* lupus mice. *Proc. Natl. Acad. Sci. USA.* 83:7018.
18. Ohga, S., Y. Yoshikai, K. Kishihara, G. Matsuzaki, T. Asano, and K. Nomoto. 1989. Expression and sequences of T cell receptor beta-chain variable genes in the enlarged lymph nodes of C57BL/6-*lpr/lpr* mice. *Clin. Exp. Immunol.* 77:130.
19. Watanabe-Fukunaga, R., C.I. Brannan, N.G. Copeland, N.A. Jenkins, and S. Nagata. 1992. Lymphoproliferation disorder in mice explained by defects in *Fas* antigen that mediates apoptosis. *Nature (Lond.).* 356:314.
20. Pisetsky, D.S., and D.V. Peters. 1981. A simple enzyme linked immuno-absorbant assay for antibodies to DNA. *J. Immunol. Methods.* 41:187.
21. Sambrook, J., E.F. Fritsch, and T. Maniatis. 1989. Molecular Cloning: A Laboratory Manual. Cold Spring Harbor Laboratory, Cold Spring Harbor, NY.
22. Frielle, T., S. Collins, K.W. Daniel, M.G. Caron, R.J. Lefkowitz, and B.K. Kobilka. 1987. Cloning of the cDNA for the human β_1-adrenergic receptor. *Proc. Natl. Acad. Sci. USA.* 84:7920.
23. Blank, R.D., G.R. Campbell, A. Calabro, and P. D'Eustachio. 1988. A linkage map of mouse chromosome 12. *Genetics.* 120:1073.
24. Blaber, M., P.J. Isackson, and R.A. Bradshaw. 1987. A complete cDNA sequence for the major epidermal growth factor binding protein in the male mouse submandibular gland. *Biochemistry.* 26:6742.
25. Bell, G.I., R.F. Santerre, and G.T. Mullenbach. 1983. Hamster preproglucagon contains the sequence of glucagon and two related peptides. *Nature (Lond.).* 302:716.
26. Johnson, K.R., S.A. Cook, M. Burstin, and M.T. Davisson. 1992. Genetic mapping of the murine gene and fourteen related sequences encoding chromosomal protein HMG. *Mammalian Genome.* In press.
27. Affholter, J.A., C.-L. Hsieh, U. Francke, and R.A. Roth. 1990. Insulin-degrading enzyme: stable expression of the human complementary DNA, characterization of its protein products, and chromosomal mapping of the human and mouse genes. *Mol. Endocrinol.* 4:1125.
28. Marcu, K.B., J. Banerji, N.A. Penncavage, R. Lang, and N. Arnhein. 1980. 5' Flanking region of immunoglobulin heavy chain constant region genes displays length heterogeneity in germlines of inbred mouse strains. *Cell.* 22:187.
29. Cullen, B.R. 1986. Trans-Activation of human immunodeficiency virus occurs via a bimodal mechanism. *Cell.* 46:973.
30. Casey, G., R. Smith, D. McGillivray, G. Peters, and C. Dickson. 1986. Characterization and chromosome assignment of the human homolog of *int*-2, a potential proto-oncogene. *Mol. Cell. Biol.* 6:502.
31. Elliott, R.W. 1987. Map locations for laminin subunits B1 and B2. *Mouse News Lett.* 78:74.
32. Chen, C.-Y., G. Salles, M.F. Seldin, A.E. Kister, E.L. Reinherz, and M.A. Shipp. 1992. Murine common acute lymphoblastic leukemia antigen (CD10 neutral endopeptidase 24.11): Molecular characterization, chromosomal localization and modeling of the active site. *J. Immunol.* 148:2817.
33. Levanon, D., C.-L. Hsieh, U. Francke, P.A. Dawson, N.D. Ridgway, M.S. Brown, and J.L. Goldstein. 1990. cDNA cloning of human oxysterol-binding protein and localization of the gene to human chromosome 11 and mouse chromosome 19. *Genomics.* 7:65.
34. Ko, H., P. Fast, W. McBride, and L.M. Staudt. 1986. A human protein specific for the immunoglobulin octamer DNA motif contains a functional homeobox domain. *Cell.* 55:135.
35. Coussens, L., P.J. Parker, L. Rhee, T.L. Yang-Fen, E. Chen, M.D. Waterfield, U. Francke, and A. Ullrich. 1986. Multiple distinct forms of bovine and human protein kinase C suggest diversity in cellular signaling pathways. *Science (Wash. DC).* 233:859.
36. Uhler, M., E. Herbert, P. D'Eustachio, and F.D. Ruddle. 1983. The mouse genome contains two nonallelic pro-opiomelanocortin genes. *J. Biol. Chem.* 258:9444.
37. Agrawal, M.G., and L.H. Bowman. 1987. Transcriptional and translational regulation of ribosomal protein formation during mouse myoblast differentiation. *J. Biol. Chem.* 262:4868.
38. Baron, B., P. Metezeau, H. Kiefer-Gachelin, and M.E. Goldberg. 1990. Construction and characterization of a DNA library from mouse chromosome 19 purified by flow cytometry. *Biol. Cell.* 69:1.
39. Watanabe-Fukunaga, R., C.I. Brannan, N. Itoh, S. Yonehara, N.G. Copeland, N.A. Jenkins, and S. Nagata. 1992. The cDNA structure, expression, and chromosomal assignment of the mouse *Fas* antigen. *J. Immunol.* 148:1274.
40. Gunning, P., P. Ponte, H. Okayama, J. Engel, H. Blau, and L. Kedes. 1983. Isolation and characterization of full-length cDNA clone for human alpha-, beta-, and gamma-actin mRNAs: skeletal but not cytoplasmic actins have an amino-terminal cysteine that is subsequently removed. *Mol. Cell.*

Biol. 3:787.
41. Lander, E.S., P. Green, J. Abrahamson, A. Barlow, M. Daly, S. Lincoln, and L. Newburg. 1987. MAPMAKER: an interactive computer package for constructing genetic linkage maps of experimental and natural populations. *Genomics.* 1:174.
42. Lander, E.S., and D. Botstein. 1989. Mapping Mendelian factors underlying quantitative traits using RFLP linkage maps. *Genetics.* 121:185.
43. Guenet, J.-L. 1992. Mouse chromosome 19. *Mammalian Genome.* 3:S266.
44. Wright, S. 1968. Evolution and the genetics of populations: a treatise in three volumes. Vol. I. *In* Genetic and Biometric Foundations. *University of Chicago Press*, Chicago. 373–420.
45. Itoh, N., S. Yonehara, A. Ishii, M. Yonehara, S.-I. Mizushima, M. Sameshima, A. Hase, Y. Seto, and S. Nagata. 1991. The polypeptide encoded by the cDNA for human cell surface antigen fas can mediate apoptosis. *Cell.* 66:233.
46. Perkins, D.L., R.M. Glaser, C.A. Mahon, J. Michaelson, and A. Marshak-Rothstein. 1990. Evidence for an intrinsic B cell defect in *lpr/lpr* mice apparent in neonatal chimeras. *J. Immunol.* 145:549.
47. Sobel, E.S., T. Katagiri, K. Katagiri, S.C. Morris, P.L. Cohen, and R.A. Eisenberg. 1991. An intrinsic B cell defect is required for the production of autoantibodies in the *lpr* model of murine systemic autoimmunity. *J. Exp. Med.* 173:1441.
48. Carlsten, H., and A. Tarkowski. 1989. Expression of heterozygous *lpr* gene in MRL mice. *Scand. J. Immunol.* 30:457.
49. Edwards, M.D., C.W. Stuber, and J.F. Wendel. 1987. Molecular-marker-facilitated investigation of quantitative-trait loci in maize. I. Numbers, genomic distribution and types of gene action. *Genetics.* 116:113.
50. Paterson, A.H., E.S. Lander, J. Hewitt, S. Peterson, and S.D. Tanksley. 1988. Resolution of quantitative traits into Mendelian factors by using a complete RFLP linkage map. *Nature (Lond.).* 335:721.
51. Todd, J.A., T.J. Aitman, R.J. Cornall, S. Ghosh, J.R.S. Hall, C.M. Hearne, A.M. Knight, J.M. Love, M.A. McAleer, J. Prins, N. Rodriques, M. Lathrop, A. Pressey, N.H. Delarato, L.B. Peterson, and L.S. Wicker. 1991. Genetic analysis of autoimmune type 1 diabetes mellitus in mice. *Nature (Lond.).* 351:542.
52. Jacob, H.J., K. Lindpaintner, S.E. Lincoln, K. Kusumi, R.K. Bunker, Y.-P. Mao, D. Ganten, V.J. Dzau, and E.S. Lander. 1991. Genetic mapping of a gene causing hypertension in the stroke-prone spontaneously hypertensive rat. *Cell.* 67:213.
53. Rise, M.L., W.N. Frankel, J.M. Coffin, and T.N. Seyfried. 1991. Genes for epilepsy mapped in the mouse. *Science (Wash. DC).* 253:669.
54. Okuda, S., L.R. Languino, E. Ruoslahti, and W.A. Border. 1990. Elevated expression of transforming growth factor-β and proteoglycan production in experimental glomerulonephritis. Possible role in expansion of the mesangial extracellular matrix. *J. Clin. Invest.* 86:453.
55. Racke, M.K., S. Dhib-Jalbut, B. Cannella, P.S. Albert, C.S. Raine, and D.E. McFarlin. 1991. Prevention and treatment of chronic relapsing experimental allergic encephalomyelitis by transforming growth factor-β1. *J. Immunol.* 146:3012.
56. Saunders, A.M., and M.F. Seldin. 1990. A molecular genetic linkage map of mouse chromosome 7. *Genomics.* 8:524.
57. Dickinson, M.E., M.S. Kobrin, C.M. Silan, D.M. Kingsley, M.J. Justice, D.A. Miller, J.D. Ceci, L.F. Lock, A. Lee, A.M. Buchberg, L.D.A. Siracusa, K.M. Lyons, R. Derynck, B.L.M. Hogan, N.G. Copeland, and N.A. Jenkins. 1990. Chromosomal localization of seven members of the murine TGF-β superfamily suggests close linkage to several morphogenetic mutant loci. *Genomics.* 6:505.
58. Ghatak, S., K. Sainis, F.L. Owen, and S.K. Datta. 1987. T-cell-receptor β and I-Aβ-chain genes of normal SWR mice are linked with the development of lupus nephritis in NZB × SWR crosses. *Proc. Natl. Acad. Sci. USA.* 84:1.
59. Babcock, S.K., V.B. Appel, M. Schiff, E. Palmer, and B.L. Kotzin. 1989. Genetic analysis of the imperfect association of H-2 haplotype with lupus-like autoimmune disease. *Proc. Natl. Acad. Sci. USA.* 86:7552.
60. Nadeau, J.H., M.T. Davisson, D.P. Doolittle, P. Grant, A.L. Hillyard, M. Kosowsky, and T.H. Roderick. 1992. Comparative map for mice and humans. *Mammalian Genome.* 1:S463.